



ULUSLARARASI 3B YAZICI TEKNOLOJİLERİ
VE DİJİTAL ENDÜSTRİ DERGİSİ

INTERNATIONAL JOURNAL OF 3D PRINTING
TECHNOLOGIES AND DIGITAL INDUSTRY

ISSN:2602-3350 (Online)

URL: <https://dergipark.org.tr/ij3dptdi>

INVESTIGATION OF OVER OBSTACLE PERFORMANCE ANALYSIS OF AUXETIC AIRLESS TYRES

Yazarlar (Authors): Ahmet Üzün^{id}, Mevlüt Yunus Kayacan^{id*}

Bu makaleye şu şekilde atıfta bulunabilirsiniz (To cite to this article): Üzün A., Kayacan M. Y., "Investigation of Over Obstacle Performance Analysis of Auxetic Airless Tyres" *Int. J. of 3D Printing Tech. Dig. Ind.*, 7(3): 415-427, (2023).

DOI: 10.46519/ij3dptdi.1336826

Araştırma Makale/ Research Article

Erişim Linki: (To link to this article): <https://dergipark.org.tr/en/pub/ij3dptdi/archive>

INVESTIGATION OF OVER OBSTACLE PERFORMANCE ANALYSIS OF AUXETIC AIRLESS TYRES

Ahmet Üzün^a , Mevlüt Yunus Kayacan^a 

^aIsparta University of Applied Sciences, Technology Faculty, Mechanical Engineering, TURKIYE

*Corresponding Author: mevlutkayacan@isparta.edu.tr

(Received: 02.08.23; Revised: 26.09.23; Accepted: 20.11.23)

ABSTRACT

Advancing technologies are leading to the development of airless tire designs that can perform well on challenging road conditions. These designs include lattice structures, mesh structures, and periodic structures, among others. In this study, three different tire designs were analyzed using finite element analysis (FEA) to evaluate their strength and dynamic behavior. Dynamic analyses were conducted on two commercial designs and one original design with re-entrant lattice structures. The study found that these structures are versatile as they provide multiple load paths to resist deformation and failure, and they can be modified to produce different properties like stiffness and strength. The original design with re-entrant structures demonstrated mechanical properties that were twice as good as other commercial tires. Moreover, a spline-lined structure was developed, and it was discovered that a two-stage tire design could enhance strength. The analyses were conducted at specific and controlled speeds with a designated bump size. The new design demonstrated at least 66% higher impact absorption energy performance than other car tyres examined. In total, nine analyses were performed, making a significant contribution to the development of airless tire design.

Keywords: Airless tyre, Non-Pneumatic, Auxetic Lattice, New Tyre Design, FEA.

1. INTRODUCTIONS

Automobile tyres have been used for nearly 100 years in line with the basic requirements of automobiles such as damping the impacts from the road and holding the vehicle to the road. It has developed in 5 phases from the 1920s to the present day. In the two phases from 1920 to the 1960s, manufacturing was carried out to meet regional expectations by producing with local technologies. Following this process, automobile tyre production has developed rapidly with the entry of different manufacturers on a global scale. Due to the short lifetime of automobile tyres, such as 3-7 years, current studies have been interested in extending this period or recycling of automobile tyres. Improvements have been made in the area of tyre features that increase vehicle comfort and facilitate vehicle use [1-5].

Car tyres were previously designed and manufactured with two zones as inner and outer tyres. While the outer tyre was exposed to

factors such as road holding and abrasion resistance, the inner tyre provided vibration impact damping thanks to its air holding structure. More modern tubeless sealed tyre designs have been introduced due to the bursting of the inner tyre and the difficulties in tyre replacement and repair. In addition, solid tyres have been developed for some of the vehicles operating under high loads. In recent years, airless tyres have started to be produced. With the use of airless tyres, risks such as tyre blowout have been completely eliminated [6-10]. Car tyres are commonly produced with thermoplastic elastomers. However, a composite structure is formed by including different components in it. 48% elastomers, 22% black carbon, 15% metal, 5% fabric products, 8% additives and 2% different elements. Commonly used elastomers are NR (natural rubber), HDPE (high density polyethylene), LDPE (low density polyethylene), PP (poly propylene), PS (poly styrene) and PVC (poly vinyl chloride).

Polyurethane-based tyres such as TPU have also started to appear with the developing technologies [11-15].

Airless tyres are a modern type of car tyre in which the outer part is not completely closed and the concept of inside and outside is not fully formed. These tyres have an elastomer structure sitting on a metal rim. These tyres, which have topologically special structures, contain vibration and impact damping properties that air acts in pneumatic tyres. Tyre topologies vary. Uniform repetitive structures such as hexagonal, triangular, etc., auxetic structures in curvilinear form, lattice-structured forms also found in additive manufacturing, volumes with variable geometry, functionally graded zone designs, kangaroo foot-like forms based on biomimetic imitation and filamentous topologies are seen. With the use of these structures, tire weights are reduced by up to 15-20%. In addition, common damage mechanisms such as bursting and tearing of tyres in difficult terrains, rough roads and long-term use can be prevented [16-22].

Airless tyres, also known as non-pneumatic tyres, are a new type of tyre that do not require air pressure to operate. They use different geometries to provide support. Examples of airless tyre geometries include honeycomb, tweel, airless radial and closed-cell foam tyres. Each of these tyre geometries has its own advantages and disadvantages depending on the specific application and performance requirements. Honeycomb tyres are lightweight and durable, while tweel tyres are known for their high shock absorption and puncture resistance. Airless radial tyres provide an efficient and comfortable ride, while closed-cell foam tyres provide better traction and stability. Airless tyres offer several advantages, including no maintenance, better puncture resistance and improved safety. They are also environmentally friendly as they are recyclable and reduce waste [23-26].

Additive manufacturing (AM) has the potential to revolutionise tyre manufacturing, including airless tyre production. AM enables the creation of complex geometries and customised designs

that may not be possible with traditional manufacturing methods. Additive manufacturing can also enable airless tyres to be produced on demand, reducing the need for large stocks and warehouses. This can also lead to more efficient supply chains and lower transport costs. However, there are some challenges to overcome to produce airless tyres using additive manufacturing, such as material limitations and production time. The materials used for the tyres to be produced with AM need to be strong, durable and able to withstand driving stress [27-30].

In the designs made, original lattice structures are generally not preferred. When the existing studies were examined, it was seen that tire designs were made by using lattice structures. Dynamic analyses on airless car tyres have only been carried out for low speeds (commonly less than 15 km/h) [24, 31-32]. As can be understood, dynamic and mechanical analyses of airless tyres are not valid for all operating conditions of a car. In this study, commercially used designs in the literature were also analysed and compared with the original designs. The analyses were completed using the finite element method, considering the case of hitting an obstacle at variable speeds between 40-120 km/h. Thus, a unique airless car tyre with a design suitable for additive manufacturing and advanced features has been developed.

2. MATERIALS AND METHODS

Finite element analysis (FEA) was performed on three different tire designs to investigate the strength and dynamic behaviour of the tires. Dynamic finite element analysis uses the finite element method to decompose a structure into mathematical models in a simple way. Each element is defined by a low dimensional (usually triangular or quadrilateral) geometric shape. By combining these elements, the structure model is created [31,33]. Dynamic analyses were performed with two different commercial tire designs and one unique design. The solid models of three different tires are shown in Figure 1.

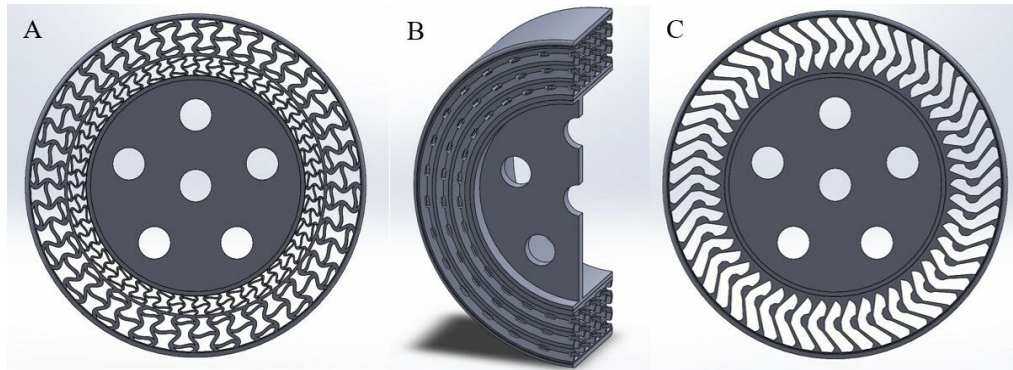


Figure 1. A) Novel design, B) commercial design “a” and C) commercial design “b”

In the original design, design criteria such as strength (energy absorption capability, etc.), ease of fabrication and originality were determined. Re-entrant lattice structures have a repeating pattern of interconnected cells with high stiffness and strength-to-weight ratios. The cells in the lattice structure are designed to provide multiple load paths that provide greater resistance to deformation and failure. The geometry of the re-entrant lattice structures can

be modified to produce different properties such as stiffness and strength, making them versatile [7,34]. By using re-entrant structure in the original design, it was found that it would provide 2 times better mechanical properties than other commercial tires. Figure 2 shows the technical drawing of the original design tire structure. (Units of measurement are given in "mm").

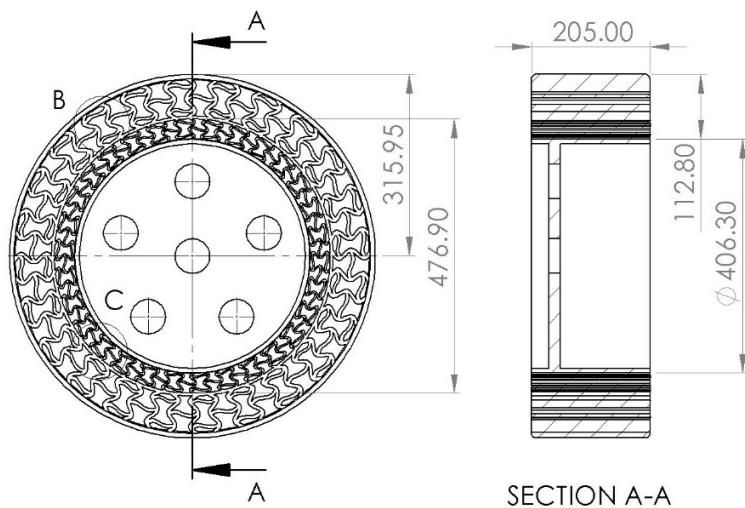


Figure 2. Technical drawing of the original design

Re-entrant structure was originalised and a spline structure was designed. The design was applied on the tire. As a result of the research, it was determined that a two-stage tire design would provide a positive effect in terms of strength [35-37]. The design was made by placing two different sized spline based re-entrant structures in the inner and outer regions. Figure 3 shows the detail pictures of the tyre structure in the outer and inner regions.

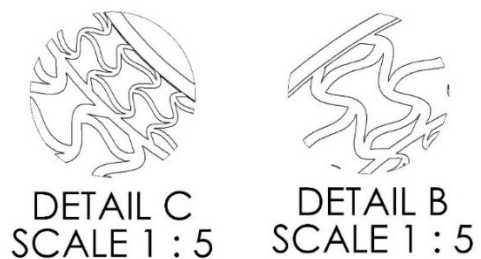


Figure 3. Detail views; B) outer zone tyre structure, C) inner zone tyre structure

Road conditions were determined for the analyses. A bump height of 50 mm was selected by analysing the bump sizes in the literature.

The tire travels on a road and passes over the bump at certain and controlled speeds. The effects on the tire as it passes over the bump were analysed. Figure 4 shows the technical

drawing of the analysis set. (Units are given in "mm").

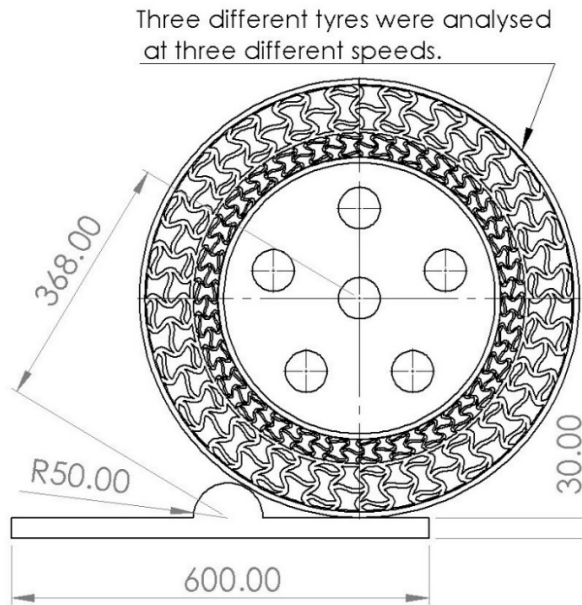


Figure 4. Technical drawing of the analysis set

Three analyses were performed for each tire. Three speeds of 40 km/h, 74 km/h and 120 km/h were used in the analyses. Rim weights were kept constant, but the weight of each tire was different. In total, 9 analyses were performed.

The variables in the analyses are tire structure, tire weights and speed. Bump size and road were kept constant in the analyses. Table 1 shows the analysis set variables.

Table 1. Analysis sets

Tyres	Lattice Structures	Weight (kg)	Velocity (km/h)
Novel Design	Spline Based Re-entrant	20 kg Tire+ 4 kg Rim	40, 74, 120
Commercial Design A	Interconnected Laminated 3D Structures	18 kg Tire + 4 kg Rim	40, 74, 120
Commercial Design B	Kangaroo Leg-like Periodic Bioinspired Lattice	19.50 kg Tire + 4 kg Rim	40, 74, 120

Preferred materials in the literature and applications were investigated. Polyurethane L135 was used as wheel material for all wheels. The density of Polyurethane L135 is 1210 kg/m³, Young's Modulus is 2410 MPa, Poisson's Ratio is 0.3897 and Shear Modulus is 867.09 MPa. AlSi10Mg alloy was used for the

wheel material. The density of AlSi10Mg alloy is 2680 kg/m³, Young's Modulus is 70000 MPa, Poisson's Ratio is 0.3, Yield Strength is 230 MPa and Tensile Strength is 345 MPa [38]. Table 2 shows the mechanical properties of Polyurethane L135, the wheel material, and AlSi10Mg, the rim material.

Table 2. Mechanical properties of materials

Tire material	Density (kg/m ³)	Young's Modulus (MPa)	Poisson's Ratio	Shear Modulus (MPa)	Yield Strength (MPa)	Tensile Strength (MPa)
Polyurethane L135	1210	2410	0.3897	867.09	-	-
Rim material AlSi10Mg	2670	70000	0.3	-	230	345

The ANSYS Workbench Explicit Dynamics module was used for the FEA. The findings led to an analysis of the levels of strain and deformation in the tire. The tire's fluctuation in speed over time was examined. Within the parameters of the investigation, the mathematical connections used with ANSYS Workbench are shown. The following Equation 1 was applied to calculate explicit dynamics using Ansys.

$$y(t_{n+1}) = y(t_n) + \Delta t \dot{y}(t_n) \quad (1)$$

The following Equation 2 was used to calculate the damage processes of the materials in the impact testing using the equation of state (EOS) principle [39].

$$P = K_1\mu + K_2\mu^2 + K_3\mu^3 \quad (2)$$

The time steps required based on the unit mesh size were calculated using Equation 3 for the Courant-Friedrichs-Lewy (CFL) case. "h" is characteristic length of a finite elements, "c" is wave speed in the material, "f" is safety factor as $f \leq 1$.

$$\Delta t \leq f \left[\frac{h}{c} \right]_{min} \quad (3)$$

Materials in accordance with Equation 4 were given a value for the longitudinal wave speed. "E" is Young's modulus and "ρ" is density [40].

$$c = \sqrt{\frac{E}{\rho}} \quad (4)$$

In general, eigenvalue techniques were employed in the modal analysis calculations in accordance with Equation 5. [M] is mass matrix

and [K] is stiffness matrix. $[K] - \omega_i^2[M]$ is definiton of natural frequencies and $\{\varphi\}_i$ is mode shapes.

$$[K] - \omega_i^2[M]\{\varphi\}_i = \{0\} \quad (5)$$

Existing equations in the literature have been developed in order to calculate the amount of energy that can be absorbed by the tyre during the passage of automobile tyres over obstacles. "m_{ty}" is weight of tire, "v" is speed of tyres, "V" is volume of tire, E is elastic modulus and "ε_{ty}" is strain of parts. "δ_{sd}" is car time sidewall deformation due to impact of the barrier. "L_{sd}" is car tire sidewall. "δ_{comp}" is compressional deformation only on sidewall. "δ_{tot}" is total deformation on sidewall [41].

$$\frac{1}{2} m_{ty} (v_{1,ty}^2 - v_{2,ty}^2) = \frac{1}{2} V_{ty} E_{TPU} \epsilon_{ty}^2 + E_{ab} \quad (6)$$

$$\epsilon_{ty} = \frac{\delta_{sd}}{L_{sd}} \quad (7)$$

$$\delta_{sd} = \delta_{tot} - \delta_{comp} \quad (8)$$

3. RESULTS AND DISCUSSIONS

In this study, three different airless car tyres with different geometries are analysed while passing over obstacles at 3 different speeds. Three moments of the original design are shown during the passage over the obstacle for three different speeds. For each speed value, three critical moments were determined. The last moment was determined as the most deformed state. As the speed increased, the amount of crushing of the wheel increased. In Figure 5, the critical moments in the analyses of the original design are given separately for each speed.

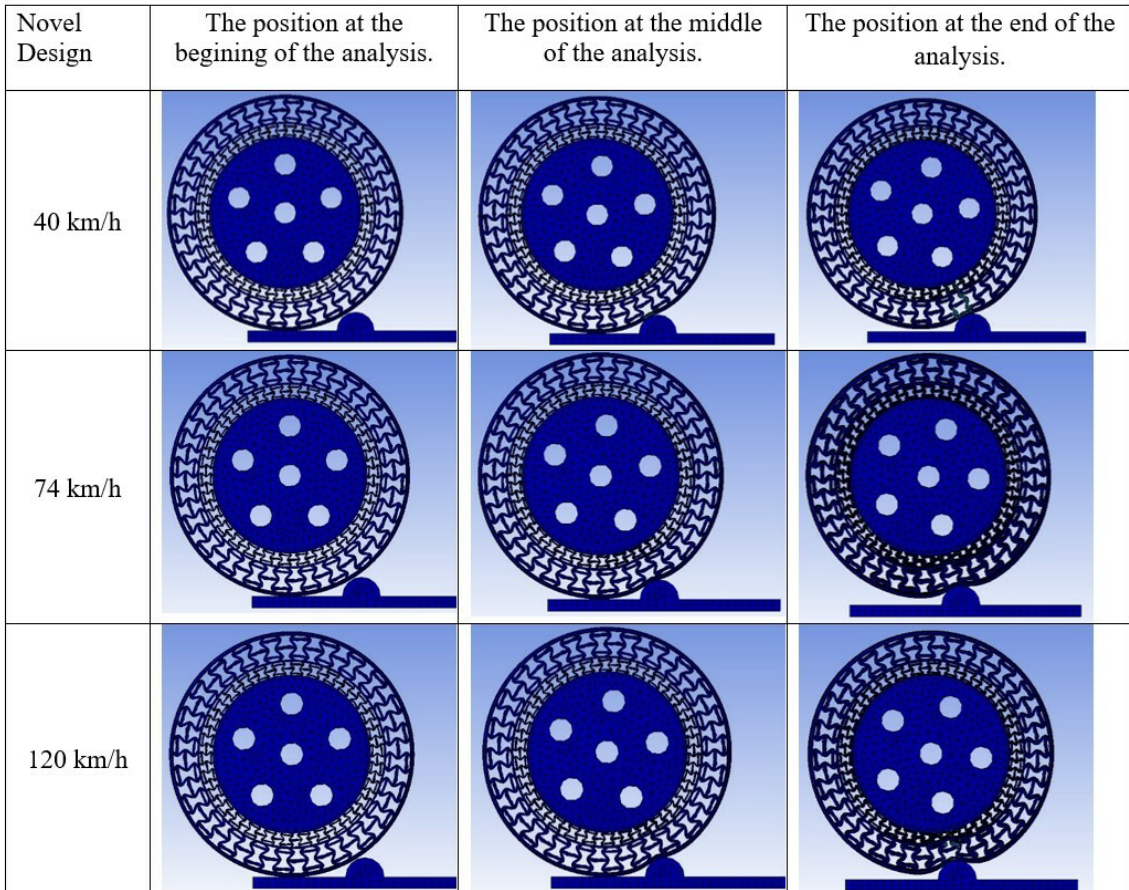


Figure 5. Moments of analysis of the original airless tyre design

40 km/h initial speed of the commercial designs and the original design are given in Figure 6. The lowest speed drop of 10% is observed in the commercial B wheel. The reason for this is that the wheel does not absorb the impact from the road. The reason why this is a disadvantage for the wheel is that it transmits the excessive load

on the wheel to the rim at variable loads. The design showing the highest speed reduction with 40% is the original design. Although speed reduction is considered as a disadvantage in terms of efficiency for automobiles, it has important advantages in terms of comfort and vehicle safety.

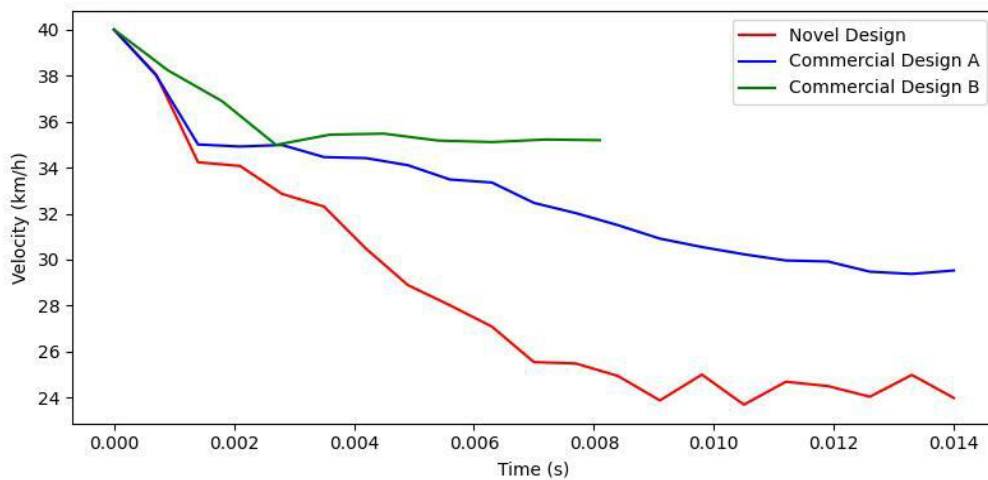


Figure 6. Speed change of wheels at 40 km/h

The highest speed reduction of approximately 16% was observed in the original design. Energy absorption was higher in the original design compared to the other wheel designs. The speed change fluctuated in the commercial B wheel, but it was observed that there was no

speed change at the last moment. In the Commercial A wheel, a 6% speed reduction occurred. Figure 7 shows the time dependent speed changes of the wheels with 74 initial speeds.

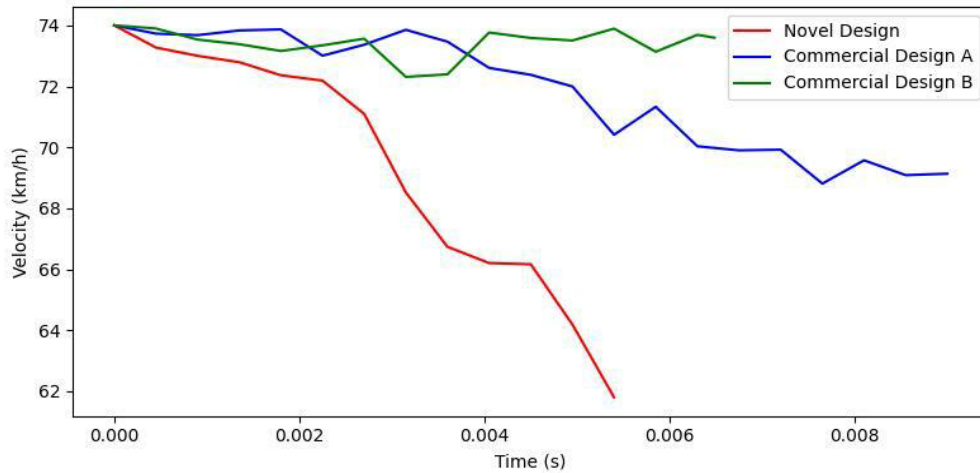


Figure 7. Speed change of the wheels at 74 km/h

With 10% speed change, the highest speed decrease was observed in the original design. In the analysis, it is observed that the percentage speed change decreases as the speed increases. Even at high speeds, the original design transfers sudden loads to the rim approximately

2 times less than commercial wheels. Therefore, it is observed that the efficiency of the original design increases at high speeds. Figure 8 shows the time-dependent speed changes of the commercial designs and the original design with an initial speed of 120 km/h.

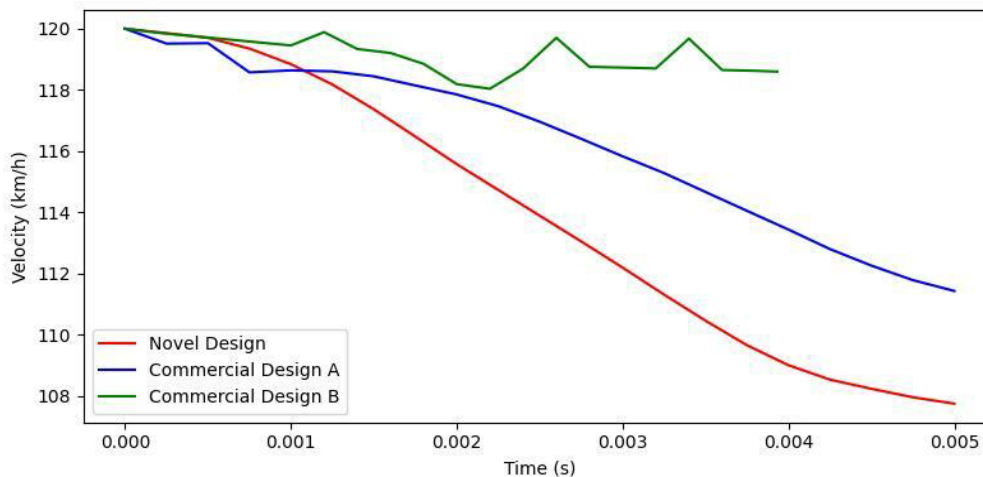


Figure 8. 120 km/h speed change of the wheels

The highest strain value of approximately 0.091 was observed in commercial design A. The original design showed a maximum strain value of 0.085. In commercial design B, the strain value remained lower than the other designs as

a result of the analysis due to the deformation of the wheel. Figure 9 shows the time-dependent strain changes of the commercial designs and the original design with an initial speed of 40 km/h.

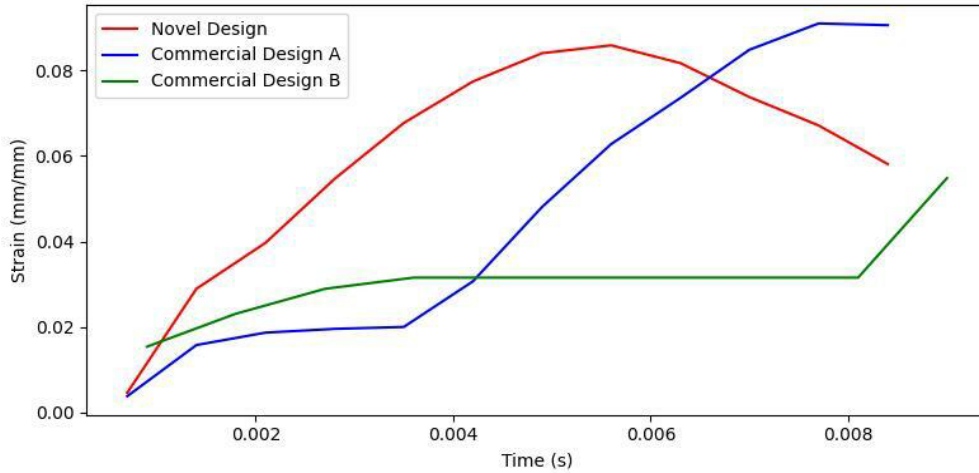


Figure 9. Strain variation of the wheels at 40 km/h speed

High strain values were observed in Novel design and commercial design. In commercial design B, the strain remained at a very limited level. As a result of the low strain capability, the possibility of permanent deformation occurred

in commercial design B. Figure 10 shows the time-dependent strain variations of the commercial designs and the original design with an initial speed of 74 km/h.

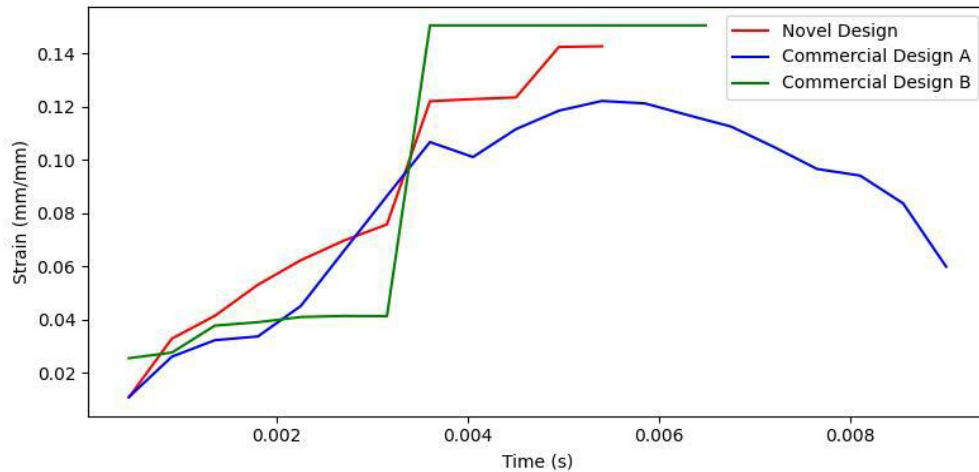


Figure 10. Strain variation of the wheels at 74 km/h speed

Novel design is the geometry with the highest strain capability. In commercial design B, permanent damage occurred at an early stage as a result of low strain capability. Commercial design A, on the other hand, showed a smoothly varying strain pattern. It is understood that

commercial design A can show a predictable deformation resistance. Figure 11 shows the time-dependent strain variations of the commercial designs and the original design with an initial speed of 120 km/h.

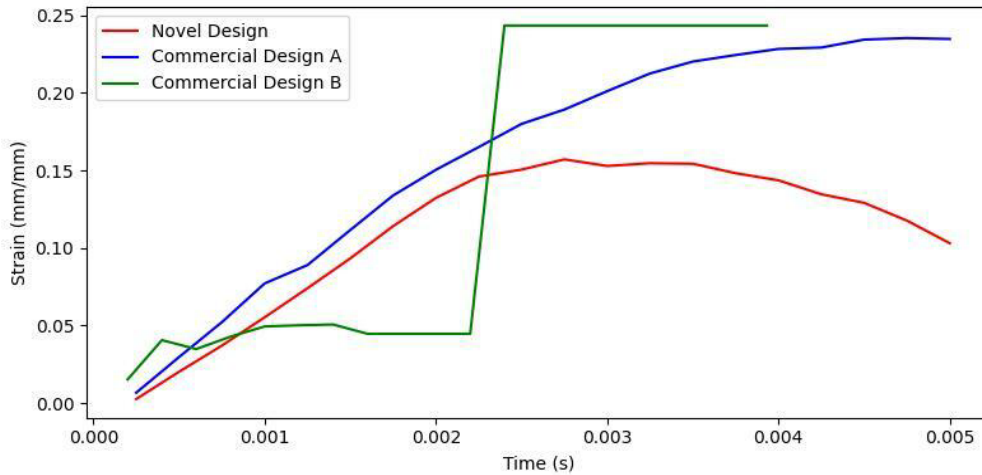


Figure 11. Strain variation of the wheels at 120 km/h speed

Similar results at 74 km/h speed were also observed for 120 km/h speed. Sudden permanent deformation occurred in commercial design B. Uniformly high strain values were measured for the original design and commercial design A. The original design was subjected to the lowest strain of the wheels, approximately 62.9 MPa. Commercial wheel B

showed the highest strain with 192 MPa. The original design showed approximately 3 times less stress than the commercial design B. The reason why less stress is observed in the original design is that the original lattice structure absorbs the energy generated by the bump. Figure 12 shows the time-dependent stress variation of the wheels at 40 km/h speed.

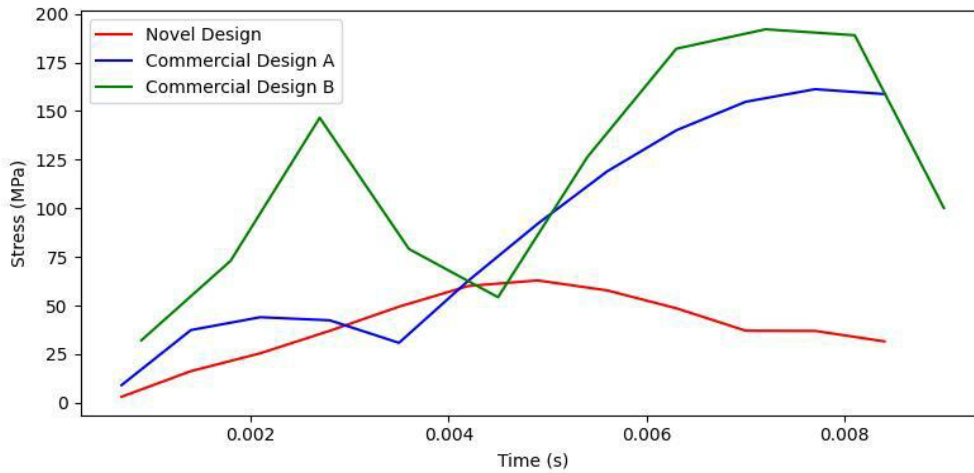


Figure 12. Stress variation of the wheels at 40 km/h speed

Commercial design B showed the highest stress with approximately 562 MPa. The original design showed a stress of 194.48 MPa. Compared to the original design, commercial design B showed about 2.2 times more stress. The maximum stress of the original design is

less than the commercial designs. As a result of the low stress values of the original design, it is in a safer position against the possibility of damage. The time-dependent stress changes of the wheels at 74 km/h speed are given in Figure 13.

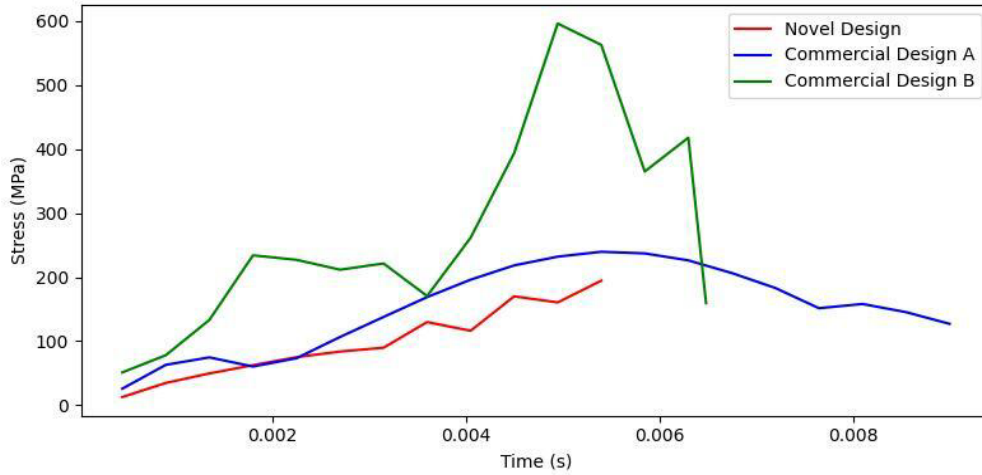


Figure 13. Stress variation of the wheels at 74 km/h speed

At 120 km/h, commercial design B was subjected to the highest stress with 492 MPa stress. The original design showed a maximum stress of 358.76 MPa and has the lowest stress

value at this speed. Figure 14 shows the time-dependent stress variations of the wheels at 120 km/h.

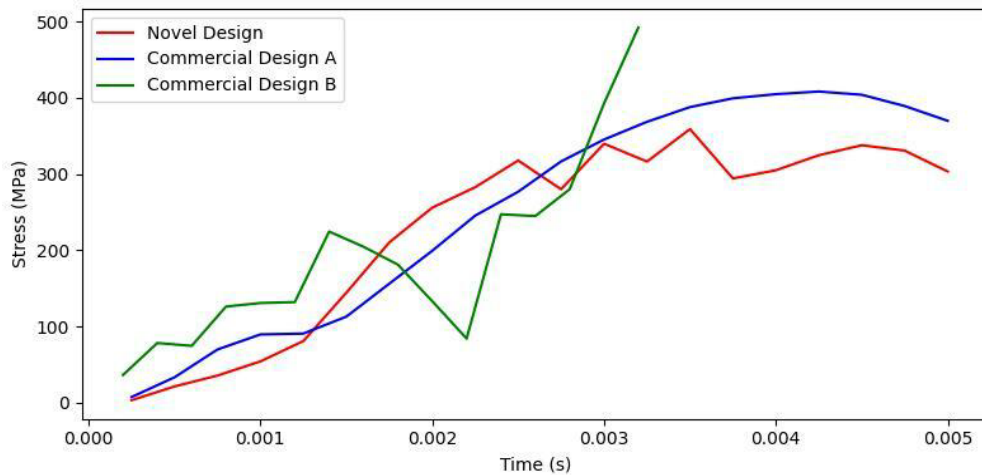


Figure 14. Stress variation of the wheels at 120 km/h speed

The stresses on the uniquely designed airless tyres are lower than those on commercial A and commercial B car tyres under all conditions. In this way, it is safe against damage formation. When examined in terms of stress and strain values, it is seen that the novel design airless

tyre is mechanically advantageous. After these, the impact energy damping capabilities of the car tyres passing over the obstacle at different speeds were calculated. As a result of the analyses, the amount of energy absorbed by the car tyres is shown in Figure 15.

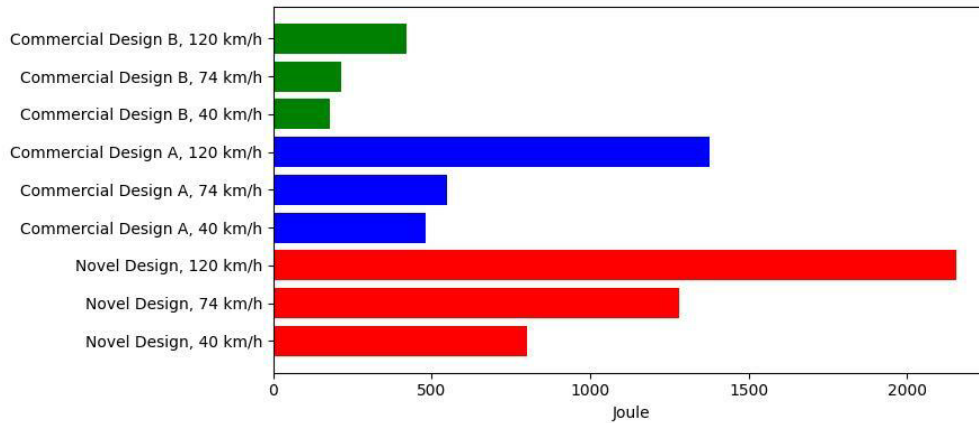


Figure 15. Energy absorbed when passing through obstacle

Looking at the amounts of absorbed energy, all car tyres absorbed a higher amount of energy at high speeds. Furthermore, novel design has at least 66% higher impact absorption energy performance than other tyres. This is a very advantageous situation in terms of passenger comfort and longevity of the car parts. As it can be understood, high performance designs can be achieved by integrating auxetic lattice structures into airless car tyres using curvilinear forms avoiding sharp edges and corners.

Compared to the studies in the literature where airless tire designs suitable for additive manufacturing were tested only under static loadings, this study investigated dynamic road conditions [42]. In addition, according to the findings obtained, it was determined that the original design showed 20% better results at low speeds compared to the design in commercial product b, which is also seen in dynamic studies in the literature [43]. The time-dependent decrease in tire speeds, especially during obstacle jumping, will significantly affect vehicle dynamic performances. However, tire efficiency started to decrease at higher speeds. Therefore, it is concluded that the developed tire design has advantages for use on uneven terrain and at low speeds.

4. CONCLUSIONS

This study analyzed commercial airless car tires along with a modern tire design that features lattice structures with variable cell sizes and an auxetic structure that can be manufactured through additive manufacturing. Finite element analysis was used to subject all tire geometries to dynamic obstacle crossing tests at different speeds. The study revealed several important findings:

- The original design showed a 40% to 100% higher speed reduction when passing over an obstacle, as the tire speed decreased to absorb the impact effect.
- The commercial B airless car tire suffered permanent damage at an early stage due to its low strain capability.
- The novel design with its high strain capability and curvilinear shaped lattice structures showed the lowest stresses.
- The novel design demonstrated at least 66% higher impact absorption energy performance than the other car tires.

It was found that the original design was not superior to existing airless tires in all aspects, but provided better performance against obstacles, especially when moving at low speeds. The shortcomings of the original design can be improved or it can be considered to be preferred only in special applications. Based on these findings, future studies can investigate the use of lattice structures with different curvilinear forms in airless car tires. Additionally, real-life obstacle jump conditions can be experimentally created for further analysis.

ACKNOWLEDGEMENTS

There are no special thank within the scope of this study.

REFERENCES

1. Mohanakumar, S., and K. Tharian George. "Impact of economic reforms on tyre industry." *Economic and political weekly*, Pages 1044-1050, 2001.

2. Klepper, Steven, and Kenneth L. Simons. "The making of an oligopoly: firm survival and technological change in the evolution of the US tire industry." *Journal of Political economy* Vol. 108, Issue 4, Pages 728-760, 2000.
3. Sienkiewicz, Maciej, et al. "Progress in used tyres management in the European Union: A review." *Waste management*, Vol. 32, Issue 10, Pages 1742-1751, 2012.
4. West, Wilhelm Joachim, and D. J. N. Limebeer. "Optimal tyre management for a high-performance race car." *Vehicle system dynamics*, Vol. 60, Issue, Pages 1-19, 2022.
5. Bowles, A. J., Fowler, G. D., O'Sullivan, C., & Parker, K. "Sustainable rubber recycling from waste tyres by waterjet: A novel mechanistic and practical analysis", *Sustainable materials and technologies*, Vol. 25, Issue 00173, 2020.
6. Nakajima, Yukio. "Application of optimisation technique to tyre design." *International journal of vehicle design* Vol. 43, Issue 1-4, Pages 49-65, 2007.
7. Jafferson, J. M., and Hemkar Sharma. "Design of 3D printable airless tyres using NTopology." *Materials Today: Proceedings*, Vol. 46, pages 1147-1160, 2021.
8. Deng, Y., Wang, Z., Shen, H., Gong, J., & Xiao, Z., "A comprehensive review on non-pneumatic tyre research", *Materials & Design*, Vol. 111742, 2023.
9. Chicu, N., Prioteasa, A. L., & Deaconu, A., "Current trends and perspectives in tyre industry", *Studia Universitatis Vasile Goldiş Arad, Seria Ştiinţe Economice*, Vol. 30, Issue 2, Pages 36-56, 2020.
10. Hoever, Carsten. *The influence of modelling parameters on the simulation of car tyre rolling losses and rolling noise*. Chalmers Tekniska Hogskola (Sweden), 2012.
11. Karger-Kocsis, J., L. Mészáros, and T. Bárány. "Ground tyre rubber (GTR) in thermoplastics, thermosets, and rubbers." *Journal of Materials Science*, Vol. 48, Pages 1-38, 2013.
12. Sienkiewicz, Maciej, et al. "Environmentally friendly polymer-rubber composites obtained from waste tyres: A review." *Journal of cleaner production*, Vol. 147, Pages 560-571, 2017.
13. Danon, Bart, and Johann Görgens. "Determining rubber composition of waste tyres using devolatilisation kinetics." *Thermochimica acta*, Vol. 621, Pages 56-60. 2015.
14. Hirata, Y., H. Kondo, and Y. Ozawa. "Natural rubber (NR) for the tyre industry." *Chemistry, manufacture and applications of natural rubber*. Woodhead Publishing, Pages 325-352, 2014.
15. Khalid, H. A., and I. Artamendi. "Mechanical properties of used-tyre rubber." *Proceedings of the Institution of Civil Engineers-Engineering Sustainability*, Vol. 157, Issue 1, 2004.
16. Khatri, S., Balaji, R., Sandeep, P. R., & Harshavardhan, K. H., "Analysis & comparative study of advance airless tyre with combination of newly designed rim". In *AIP Conference Proceedings*, Vol. 2317, Issue 1, 2021.
17. Ramakrishnan, T. "Design optimization of Airless Tyre-Numerical Approach". In *IOP Conference Series: Materials Science and Engineering*, Vol. 1057, Issue 1, Issue 012032, 2021.
18. Rugsaj, R., & Suvanjumrat, C. "Mechanical characteristics of airless tyre by laboratory testing". In *IOP Conference Series: Materials Science and Engineering*, Vol. 773, Issue 1, Issue 012037, 2020.
19. Ott, J., & Pearlman, J. "Scoping review of the rolling resistance testing methods and factors that impact manual wheelchairs". *Journal of Rehabilitation and Assistive Technologies Engineering*, Vol. 8, Issue 2055668320980300, 2021.
20. Patel, M. D., Pappalardo, C. M., Wang, G., & Shabana, A. A. "Integration of geometry and small and large deformation analysis for vehicle modelling: chassis, and airless and pneumatic tyre flexibility". *International Journal of Vehicle Performance*, Vol. 5, Issue 1, Pages 90-127, 2019.
21. Kannan, P., Shaik, A., Kumar, Y., & Baredy, N. S. "Design analysis and 3D printing of non-pneumatic tyre". *SAE Technical Paper*. Vol. 28, Issue 0059, 2019.
22. Andriya, N., Dutta, V., & Vani, V. V. "Study on 3D printed auxetic structure-based non-pneumatic tyres (NPT'S)". *Materials and Manufacturing Processes*, Vol. 37, Issue 11, Pages 1280-1297, 2022.
23. Bras, B., & Cobert, A. "Life-cycle environmental impact of Michelin Tweel® tire for passenger vehicles". *SAE international journal of passenger cars-mechanical systems*, Vol. 4, Issue 93, Pages 32-43, 2011.
24. Jin, X., Hou, C., Fan, X., Sun, Y., Lv, J., & Lu, C. "Investigation on the static and dynamic behaviors of non-pneumatic tires with honeycomb

spokes”. *Composite Structures*, Vol. 187, Pages 27-35, 2018.

25. Periasamy, K., & Vijayan, S. “Design and development of air-less car tire”. *International Journal of Advances in Engineering & Technology*, Vol. 7, Issue 4, Issue 1312, 2014.

26. Phumnok, E., Boonphang, J., & Bourkaew, O. “Effect of filler types on properties of the natural rubber closed cell foam”. *Applied Mechanics and Materials*, Vol. 886, Pages 213-218, 2019.

27. Sardinha, M., Reis, L., Ramos, T., & Vaz, M. F. “Non-pneumatic tire designs suitable for fused filament fabrication: an overview. *Procedia Structural Integrity*, Vol. 42, Pages 1098-1105, 2022.

28. Vicente, C. M., Sardinha, M., Reis, L., Ribeiro, A., & Leite, M. “Large-format additive manufacturing of polymer extrusion-based deposition systems: review and applications”. *Progress in Additive Manufacturing*, Pages 1-24, 2023.

29. Herzberger, J., Sirrine, J. M., Williams, C. B., & Long, T. E. “Polymer design for 3D printing elastomers: recent advances in structure, properties, and printing”. *Progress in Polymer Science*, Vol. 97, Issue 101144, 2019.

30. Wang, J., Yang, B., Lin, X., Gao, L., Liu, T., Lu, Y., & Wang, R. “Research of TPU materials for 3D printing aiming at non-pneumatic tires by FDM method”. *Polymers*, Vol. 12, Issue 11, Issue 2492, 2020.

31. Rugsaj, R., & Suvanjumrat, C. “Dynamic finite element analysis of rolling non-pneumatic tire”. *International Journal of Automotive Technology*, Vol. 22, Pages 1011-1022, 2021.

32. Genovese, A., Garofano, D., Sakhnevych, A., Timpone, F., & Farroni, F. “Static and dynamic analysis of non-pneumatic tires based on experimental and numerical methods”. *Applied Sciences*, Vol. 11, Issue 23-11232, 2021.

33. Li, H., Zhou, H., Yang, J., Ge, J., Wang, G., & Xu, T. “Study of the dynamic performance of rolling non-pneumatic tires using finite element method”. *Journal of the Brazilian Society of Mechanical Sciences and Engineering*, Vol. 44, Issue 7, Issue 289, 2022.

34. A.N. Biswas, N. Mahesh, S.R. Peri, B.R. Krishnan, and P.R. Sreekanth, Hybrid auxetic materials implemented in crates & non-pneumatic tires for shock absorption, *Materials Today: Proceedings*, Vol. 56, Pages 1327-1334, 2022.

35. Biswas, A. N., Mahesh, N., qPeri, S. R., Krishnan, B. R., & Sreekanth, P. R. Hybrid auxetic materials implemented in crates & non-pneumatic wheels for shock absorption”. *Materials Today: Proceedings*, Vol. 56, Pages 1327-1334, 2022.

36. Liu, B., & Xu, X. “Mechanical behavior and mechanism investigation on the optimized and novel bio-inspired nonpneumatic composite tire”s. *Reviews on Advanced Materials Science*, Vol. 61, Issue 1, Pages 250-264, 2022.

37. Zang, L., Wang, X., Yan, P., & Zhao, Z. “Structural design and characteristics of a non-pneumatic tire with honeycomb structure”. *Mechanics of Advanced Materials and Structures*, Vol. 29, Issue 25, Pages 4066-4073, 2022.

38. Arjunan, A., Singh, M., Baroutaji, A., & Wang, C. “Additively manufactured AlSi10Mg inherently stable thin and thick-walled lattice with negative Poisson’s ratio”. *Composite Structures*, Vol. 247, Issue 112469, 2020.

39. Marx, J., Portanova, M., & Rabiei, A. “Ballistic performance of composite metal foam against large caliber threats”. *Composite structures*, Vol. 225, Issue 111032, 2020.

40. Lin, Y. F., Ye, J. W., & Lo, C. M. “Application of impact-echo method for rockbolt length detection”. *Construction and Building Materials*, Vol. 316, Issue 125904, 2022.

41. Satkar, A. R., Mache, A., & Kulkarni, A. “Numerical investigation on perforation resistance of glass-carbon/epoxy hybrid composite laminate under ballistic impact”. *Materials Today: Proceedings*, Vol. 59, Pages 734-741, 2022.

42. Andriya, N., Dutta, V., & Vani, V. V. “Study on 3D printed auxetic structure-based non-pneumatic tyres (NPT’S)”. *Materials and Manufacturing Processes*, Vol. 37, Issue 11, Pages 1280-1297, 2022.

43. Liang, X., Fu, H., Wang, Y., Ku, L., Qiao, H., & Li, N. “Study of composite load-bearing characteristics of the Uptis non-pneumatic tyre”. *International Journal of Vehicle Systems Modelling and Testing*, Vol. 16, Issue 1, Pages 79-93, 2022.